This article has been accepted for publication in a future issue of this journal, but has not been fully edited. Content may change prior to final publication. Citation information: DOI 10.1109/LED.2019.2954326, IEEE Electron Device Letters

Equivalent Circuit of Quantum-Dot LED and Acquisition of Carrier Lifetime in Active Layer

Hua Xiao, Kai Wang, *Member, IEEE*, Rui Wang, *Member*, *IEEE*, Wanli Chen, and Kin Seng Chiang, *Senior Member*, *IEEE*

***Abstract*—We propose an equivalent circuit for a quantum-dot LED (QLED), where the resistances and the capacitances are expressed in terms of the physical parameters of the QLED. The validity of the equivalent circuit is verified by measurement results. From the measured frequency response of the QLED and the calculated frequency response of the equivalent circuit, we are able to deduce the carrier lifetime in the active layer of the QLED. The availability of the equivalent circuit can facilitate the analysis of the electrical characteristics of QLEDs.**

***Index Terms*—Quantum-dot light-emitting diode, equivalent circuit, frequency response, carrier lifetime.**

I. Introduction

Electroluminescent (EL) quantum-dot (QD) LEDs (QLEDs) are promising light sources for display and illumination for their inkjet processability, high color tunability, and high color purity [1]. Their large bandwidths [2], compared with those of other solution-processed light sources, also render them suitable for communication applications. In this paper, we propose an equivalent circuit for the analysis of QLEDs and demonstrate the evaluation of the carrier lifetime in the active layer of the QLED with the help of the equivalent circuit.

Equivalent circuits have been proposed for semiconductor LEDs [3] and organic LEDs (OLEDs) [4]–[6] to facilitate the analysis of the electrical characteristics of these devices. These equivalent circuits are mostly developed by fitting the values of the circuit components with measured electrical characteristics of the devices. As such, the circuits are not directly related to the physical structures and the materials of the devices. Besides, some DC models [5] do not allow the evaluation of the modulation characteristics of the device. There is no equivalent circuit specifically developed for QLEDs.

The equivalent circuit we propose for a QLED reflects the physical structure of the device, where the component values are expressed in terms of the physical parameters of the device. Compared with reported equivalent circuits of OLEDs [4]–[6], our circuit allows a more direct and accurate evaluation of the roles of different layers of the device on its electrical characteristics. The validity of our circuit is verified with measured electrical characteristics. By measuring the frequency response of the QLED and with the effect of the equivalent circuit deducted, we are able to obtain the carrier lifetime in the active layer of the QLED. Carrier lifetime in the active layer, namely the lifetime of carriers that exist in the QD layer before recombination, is an important parameter of QLED, as it directly reflects the recombination process and the electron-hole dynamics in the active layer [7]. Existing methods for measuring carrier lifetimes in semiconductor structures, such as those based on the measurements of photoluminescence decay [8] and open-circuit voltage decay [9], could be applied to a QLED, but the result includes all the effects from the injection and transport layers of the QLED. There is no method reported for direct measurement of the carrier lifetime in the active layer of a QLED. Our approach provides a simple way to find this important parameter.

II. Development of Equivalent Circuit

Figure 1(a) shows the structure of a 4-mm^2 CdSe/ZnS QLED considered in our study, which consists of the following layers: indium tin oxide (ITO, 100 nm) / poly(3.4-ethylene-dioxythiophene) polystyrene sulfonate (PEDOT:PSS, 40 nm) / poly (9,9-dioctylfluorene-co-N-(4-(3-methylpropyl)) diphenyl-amine) (TFB, 29 nm) / CdSe/ZnS QDs (18 nm) / Zinc Oxide (ZnO, 33 nm) / Al (100 nm). The ITO, PEDOT:PSS, TFB, QD, ZnO, and Al layers serve as the anode, the hole injection layer (HIL), the hole transport layer (HTL), the emitting layer, the electron transport layer (ETL), and the cathode, respectively. The thicknesses were measured with a Bruker Stylus Profiler. This QLED emitted red light at a wavelength of 634 nm with a full-width-at-half-maximum (FWHM) of 22 nm. Details on the measurement of the optical properties and the frequency response of the QLED are given in [2]. Figure 1(b) shows the energy level diagram of the QLED [2]. In our experiments, a DC bias voltage (or an input voltage) varying from 3 to 10 V was applied to the QLED. For the measurement of the frequency response of the device, a sinusoidal signal with an amplitude of 1V was superimposed on the DC bias.

Figure 1(c) shows the proposed circuit of the forward-biased QLED and Fig. 1(d) shows the correspondence between the circuit components and the physical layers of the device.

Manuscript received xxx, 2019. This work was supported in part by the National Key Research and Development Program (No.2017YFE0120400), National Natural Science Foundation of China (No. 61875082), Natural Science Foundation of Guangdong (No.2017B030306010), Guangdong Province's Key R&D Program (No. 2019B010924001) , and Shenzhen Innovation Project (No. JSGG20170823160757004). (Corresponding authors: Kai Wang and Rui Wang)

H. Xiao and K. S. Chiang are with the Department of Electrical Engineering, City University of Hong Kong, Hong Kong SAR, China (email: xiaocherry89@gmail.com; eeksc@cityu.edu.hk)

K. Wang, W. Chen, and R. Wang are with the Department of Electrical and Electronic Engineering, Southern University of Science and Technology, Shenzhen, 518055, China (email: wangk@sustech.edu.cn, chenwl@sustech.edu.cn, and wangr@sustech.edu.cn).

0741-3106 (c) 2019 IEEE. Personal use is permitted, but republication/redistribution requires IEEE permission. See http://www.ieee.org/publications_standards/publications/rights/index.html for more information.

This article has been accepted for publication in a future issue of this journal, but has not been fully edited. Content may change prior to final publication. Citation information: DOI 10.1109/LED.2019.2954326, IEEE Electron Device Letters

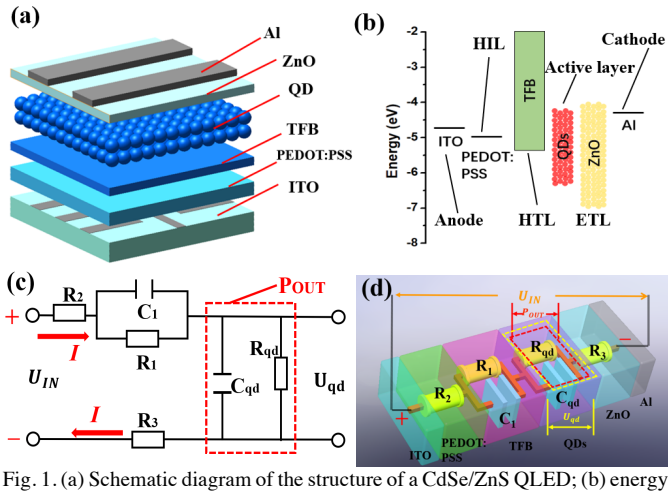

Fig. 1. (a) Schematic diagram of the structure of a CdSe/ZnS QLED; (b) energy level diagram of the QLED; (c) the proposed equivalent circuit of the QLED, and (d) the correspondence between the circuit components and the physical layers of the QLED.

The QD layer is equivalent to a parallel circuit of a forward-current-caused capacitance C_{qd} and a resistance R_{qd}. Because of the low accessibility of holes from the TFB layer into the QD layer, the stack of holes at the surface between the HTL layer and the QD layer forms an accumulated-charge-caused barrier capacitance C_1. Therefore, the TFB layer is equivalent to a parallel circuit of the barrier capacitance C_1 and a resistance R_1. These two parallel circuits are in series of the resistances of the PEDOT:PSS layer and the ZnO layer, R_2 and R_3. Because the energy gaps across Al/ZnO and ZnO/QDs are small, as shown in Fig. 1(b), electrons can be easily injected from the Al layer into the ZnO layer and the QD layer. Electron accumulation in the ZnO/QDs interface and hence the capacitance in the ZnO layer can be ignored. If necessary, electron accumulation in the ZnO/QDs interface, which may occur in blue QLEDs [10], can be taken into account by placing an accumulated-charge-caused barrier capacitance across R_3. Similarly, the capacitance in the PEDOT:PSS layer can be ignored for its high carrier mobility and good electrode contact. The resistances of the Al cathode and the ITO anode are negligible and can also be ignored.

The transfer function of the QLED, $Q(\omega)$, is given by the ratio of the emitted optical power $P_{OUT}(\omega)$ and the input voltage $U_{IN}(\omega)$, where ω is the angular modulation frequency. According to Fig. 1(c) and (d), the optical power P_{OUT} should be generated from the voltage U_{qd} across the QD layer. The electrical-optical conversion in the QLED can then be described as the conversion from U_{IN} to U_{qd} followed by the conversion from U_{qd} to P_{OUT}.

The transfer function that describes the conversion from U_{IN} to U_{qd}, denoted as $H(\omega)$, depends solely on the components in the equivalent circuit. These components consume electric power and slow down the transportation of carriers in the QLED. The conversion from U_{qd} to P_{OUT}, denoted as $F(\omega)$, takes place in the active layer of the QLED and depends on the rate of electron-hole recombination. Similar to the case of a luminescent diode, the response in the active layer depends on the carrier lifetime τ as $1/\sqrt{1+\omega^2\tau^2}$ [11], which consists of both radiative and non-radiative contributions. Therefore, with the help of the equivalent circuit, the transfer function of the QLED is obtained as

$$Q(\omega) = H(\omega)F(\omega), \tag{1}$$

with

$$H(\omega) = \frac{U_{qd}(\omega)}{U_{IN}(\omega)} = \frac{\frac{R_{qd}-j\omega {R_{qd}}^2 C_{qd}}{1+\left(\omega R_{qd}C_{qd}\right)^2}}{\frac{R_{qd}-j\omega {R_{qd}}^2 C_{qd}}{1+\left(\omega R_{qd}C_{qd}\right)^2}+\frac{R_1-j\omega {R_1}^2 C_1}{1+(\omega R_1 C_1)^2}+R_2+R_3}, \tag{2}$$

$$F(\omega) = \frac{P_{OUT}(\omega)}{U_{qd}(\omega)} = \frac{A}{\sqrt{1+\omega^2\tau^2}}, \tag{3}$$

where A is a constant.

The resistivity of each layer in the QLED is given by $\rho = \rho_0/\kappa(1-In\kappa)$ [12], where $\rho_0 = 1/ne\mu$ is the bulk resistivity, $n = J/e\mu E$ is the electron concentration with J being the current density, e the electron charge, μ the mobility of the material, and E the electric field in the layer, and κ is given by $d/2l_{bulk}$ with d being the layer thickness and l_{bulk} the bulk mean free path. The resistance of the layer is then given by $R = \rho d/S$, where $S = 4$ mm^2 is the emission area of the QLED. The values of l_{bulk} for PEDOT:PSS [13], TFB [14], QDs [15], ZnO [16] are 2.7, 3, 20, and 2.6 nm, respectively, and the values of the mobilities for ITO [17], PEDOT:PSS [18], TFB [19], QDs [20], ZnO [21], and Al are 20, 3×10^{-2}, 1.2×10^{-2}, 1.0×10^{-2}, 2.3×10^{-3}, and 10^3 cm$^2V^{-1}s^{-1}$, respectively.

The injection current density J can be measured experimentally [2], but the electric field E in each layer cannot be measured. Instead, we calculate E with the commercial software Setfos [22] – the software is widely used for the analysis of optoelectronic devices. The calculation takes into account all the QLED parameters, namely the layer thicknesses, the mobilities, the dielectric constants, and the energy levels of different layers shown in Fig. 1(b), as well as the applied voltage. Given the electric field E in each layer and the measured injection current density J, we can calculate the bulk resistivity $\rho_0 = E/J$ in each layer and hence the corresponding resistance.

The barrier capacitance caused by the space charges is given by $C_1 = (\varepsilon\varepsilon_0/\sqrt{2}L_d)\exp(-eV_{d1}/2kT)$ [23], where ε is the dielectric constant of the material, ε_0 is the permittivity of the vacuum, $L_d = \sqrt{\varepsilon kT/(e^2 n)}$ is the debye length, k is the Boltzmann coefficient, T (= 298 K) is the temperature, and V_{d1} is the potential difference between the TFB layer and the QD layer. The values of ε for PEDOT:PSS [24], TFB [24], QDs [25], ZnO [26] are 3, 3, 6, and 3.5, respectively. The amount of residual charges Q_R in the QD layer is the amount of charges Q_I in the current I minus the amount of charges Q_P consumed for photon conversion. Therefore, C_{qd} can be expressed as

$$C_{qd} = S\frac{dQ_R}{dU_{IN}} = S\frac{dQ_I}{dU_{IN}} - S\frac{dQ_P}{dU_{IN}}, \tag{4}$$

with $Q_I = It$ and $Q_P = N_e et = \frac{et}{hc}\int\frac{P(\lambda)\lambda}{\eta_{EQE}}d\lambda$, where t is the unit time, N_e is the electron number, h is Planck's constant, c is the speed of light in vacuum, η_{EQE} is the external quantum efficiency, and $P(\lambda)$ is the spectral power density of the emitted light from a packaged QLED. The effects of both radiative and non-radiative recombinations are implicitly taken into account by η_{EQE}. C_{qd} can be calculated from Eq. (4) with the

0741-3106 (c) 2019 IEEE. Personal use is permitted, but republication/redistribution requires IEEE permission. See http://www.ieee.org/publications_standards/publications/rights/index.html for more information.

This article has been accepted for publication in a future issue of this journal, but has not been fully edited. Content may change prior to final publication. Citation information: DOI 10.1109/LED.2019.2954326, IEEE Electron Device Letters

knowledge of dI/dU_{IN}, $P(\lambda)$, and η_{EQE}, which can be found experimentally [2].

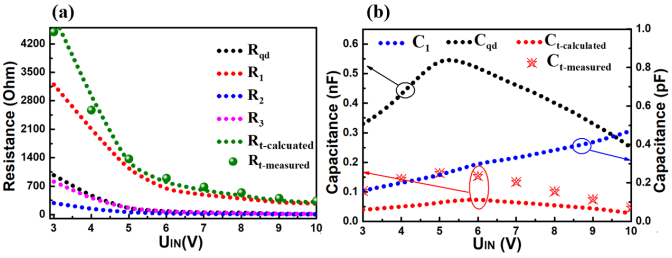

Fig. 2. (a) Values of R_{qd}, R_1, R_2, and R_3 calculated at different applied voltages and comparison between calculated and measured input resistance R_t; (b) values of C_{qd} and C_1 calculated at different applied voltages and comparison of calculated and measured input capacitance C_t.

III. Results and Discussions

Figure 2 shows the values of the resistances and the capacitances in the equivalent circuit calculated at different input voltages. As shown in Fig. 2(a), R_1 has the largest value compared with other resistances and all the resistances decrease with an increase in the applied voltage. The reason is that the electric potential changes severely between the TFB layer and the QD layer, which directly influences the values of E and R_1. As shown in Fig. 2(b), C_{qd} has a peak value at a voltage of 5.2 V and the value of C_1 increases monotonically with the applied voltage. The peak of C_{qd} is due to the balance between the speed of charge injection and the speed of charge conversion into light in the QD layer. As C_1 is inversely proportional to the carrier density, its value increases with the applied voltage. The input impedance of the circuit can be written as a resistance R_t in parallel with a capacitance C_t, where R_t is the sum of R_{qd}, R_1, R_2, and R_3.

We calculate the transfer function $H(\omega)$ of the equivalent circuit and the corresponding bandwidth B. With the knowledge of the bandwidth B and the resistance R_t, we deduce C_t from the expression $B = 1/(2\pi R_t C_t)$. We measured the values of R_t and C_t of the QLED at different DC bias voltages with a semiconductor parameter analyzer [2] and compare the measurement data with the calculated values. As shown in Fig. 2, the measured values agree well with the calculated values, which thus verifies the validity of the equivalent circuit. We measured the frequency response of the QLED, i.e., $Q(\omega)$, by varying the modulating frequency of the input sinusoidal signal at different DC bias voltages. The results are shown in Fig. 3(a). We also calculate the frequency response of the equivalent circuit $H(\omega)$ and the results are shown in Fig. 3(b).

The bandwidth of $H(\omega)$ is wider than that of $Q(\omega)$ at the same voltage. For example, at a bias voltage of 10 V, $H(\omega)$ has a bandwidth of ~20 MHz, while $Q(\omega)$ has a bandwidth of only ~8 MHz. We obtain $F(\omega)$ by dividing $Q(\omega)$ by $H(\omega)$. The results are shown by the discrete points in Fig. 3(c). By fitting the discrete points with curves in the form of $F(\omega) = 1/\sqrt{1+\omega^2\tau^2}$, we find the values of the carrier lifetime τ at different applied voltages, which are shown by the discrete points in Fig. 3(d). The carrier lifetime decreases with an increase in the applied voltage, which indicates that the response of the QLED is faster at a higher applied voltage. This finding agrees with our previous experimental study [2], where the bandwidth of a QLED is shown to be mainly limited by the carrier lifetime at a large injection current.

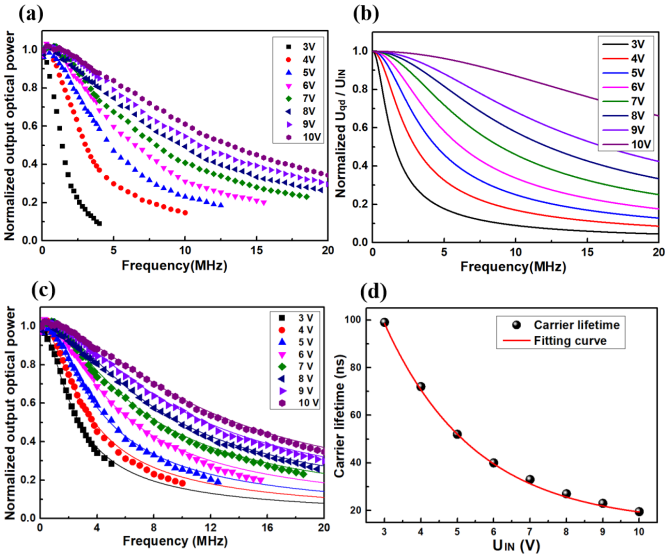

Fig. 3. (a) Measured frequency response of the QLED, $Q(\omega)$, (b) calculated frequency response of the equivalent circuit, $H(\omega)$; (c) $F(\omega)$ obtained by dividing $Q(\omega)$ by $H(\omega)$, and (d) carrier lifetime obtained by fitting the results in (c) with $F(\omega) = 1/\sqrt{1+\omega^2\tau^2}$.

IV. Conclusion

We have proposed an equivalent circuit for QLEDs, where the resistances and the capacitances are expressed in terms of the physical parameters of the device. We have measured the input resistance and capacitance of a specific QLED and the measurement data agree well with the results calculated from the equivalent circuit. We are able to deduce the carrier lifetime in the active layer of the QLED by dividing the frequency response of the device by that of the equivalent circuit. Our proposed equivalent circuit provides a convenient model for the analysis of the electrical characteristic of QLEDs within the linear operation regimes of the devices.

References

[1] R. Vasan, H. Salman, M. O. Manasreh, "Solution processed high efficiency quantum dot light emitting diode with inorganic charge transport layers," *IEEE Electr. Device L.*, vol. 39, no. 4, pp. 536-539, Apr. 2018. doi: 10.1109/LED.2018.2808679.

[2] H. Xiao, X. Xiao, D. Wu, R. Wang, K. Wang, and K. S. Chiang, "Effects of Injection current on the modulation bandwidths of quantum-dot light-emitting diodes," 2019 (accepted) IDO:10.1109/TED.2019.2941561.

[3] C. Y. Zhu, L. F. Feng, C. D. Wang, H. X. Cong, G. Y. Zhang, and Z. Z. Chen, "Negative capacitance in light-emitting devices," *Solid State Electron.*, vol. 53, no. 3, pp. 324-328, Feb. 2009. doi: 10.1016/j.sse.2009.01.002.

[4] S. Berleb, W. Brütting, and G. Paasch, "Interfacial charges in organic hetero-layer light emitting diodes probed by capacitance–voltage measurements," *Synthetic Metals*, vol. 122, no. 1, pp. 37-39, May 2001. doi: 10.1016/S0379-6779(00)01356-4.

[5] X. Jiang and C. Xu, "An electro-optical OLED model for prediction and compensation of AMOLED aging artifacts," SID Symposium Digest of Technical Papers, vol. 49, no. 1, pp. 441-444, May 2018. doi: 10.1002/sdtp.12595.

[6] S. X. Zong, C. N. Li, C. H. Lv, G. H. Xie, Y. Zhao, and S. Y. Liu, "Equivalent circuit model of top-emitting OLED for the designing of OLED-on-silicon microdisplay," Advanced Materials Research. Trans.

0741-3106 (c) 2019 IEEE. Personal use is permitted, but republication/redistribution requires IEEE permission. See http://www.ieee.org/publications_standards/publications/rights/index.html for more information.

This article has been accepted for publication in a future issue of this journal, but has not been fully edited. Content may change prior to final publication. Citation information: DOI 10.1109/LED.2019.2954326, IEEE Electron Device Letters

Tech. Publications, vol. 383, pp. 7037-7042, Nov. 2011. doi: 10.4028/www.scientific.net/AMR.383-390.7037.

[7] W. C. Fan, W. C. Chou, J. D. Lee, L. Lee, N. D. Phu, and L. H. Hoang, "Study of extending carrier lifetime in ZnTe quantum dots coupled with ZnCdSe quantum well," *Physica B: Condensed Matter*, vol. 532, pp. 195-199, Mar. 2018. doi: 10.1016/j.physb.2017.04.024.

[8] C. H. Henry, B. F. Levine, R. A. Logan, and C. G. Bethea, " Minority carrier lifetime and luminescence efficiency of 1.3 μm InGaAsP-InP double heterostructure layers," *IEEE J. Quantum Elect.*, vol.19, no. 6, pp. 905-912, Jul. 1983. doi: 10.1109/JQE.1983.1071997.

[9] Y. Arafat, M. F. Mohammedy, and M. M. S. Hassan. "Optical and other measurement techniques of carrier lifetime in semiconductors," *Int. J. Optoelectron. Eng*., vol. 2, no. 2, pp. 5-11, Jan. 2012. doi: 10.5923/j.ijoe.20120202.02.

[10] S. Chen, W. Cao, T. Liu, S. W. Tsang, Y. Yang, X. Yan, and L. Qian, "On the degradation mechanisms of quantum-dot light-emitting diodes," *Nat. Commun.*, vol. 10, no. 1, pp. 765-1-9, Feb. 2019. doi: 10.1038/s41467-019-08749-2.

[11] Y. S. Liu, and D. A. Smith, "The frequency response of an amplitude-modulated GaAs luminescence diode," *Proc. IEEE*, vol. 62, no. 3, pp. 542-544, Mar. 1975. doi: 10.1109/proc.1975.9786.

[12] F. Lacy, "Developing a theoretical relationship between electrical resistivity, temperature, and film thickness for conductors," *Nanoscale Res. Lett.*, vol. 6, no. 1, pp. 636-1-14, Dec. 2011. doi: 10.1186/1556-276X-6-636.

[13] S. I. Na, G. Wang, S. S. Kim, T. W. Kim, S. H. Oh, B. K. Yu, T. Lee, and D. Y. Kim, "Evolution of nanomorphology and anisotropic conductivity in solvent-modified PEDOT: PSS films for polymeric anodes of polymer solar cells," *J. Mater. Chem.*, vol. 19, no. 47, pp. 9045-9053, Oct. 2009. doi: 10.1039/b915756e.

[14] P. J. Cumpson, "Estimation of inelastic mean free paths for polymers and other organic materials: use of quantitative structure–property relationships," *Surf. Interface Anal.*, vol. 31, no. 1, pp. 23-34, Jan. 2001. doi: 10.1002/sia.948.

[15] M. C. Beard, G. M. Turner, and C. A. Schmuttenmaer, "Size-dependent photoconductivity in CdSe nanoparticles as measured by Time-Resolved Terahertz Spectroscopy," *Nano Lett.*, vol. 2, no. 9, pp. 983-987, Jul. 2002. doi: 10.1021/nl0256210.

[16] M. Krawczyk, W. Lisowski, J. W. Sobczak, A. Kosin´ski, and A. Jablonski, "Elastic-peak electron spectroscopy (EPES) studies of ZnO single crystals," *J. Alloy. Compd.*, vol. 590, pp. 553-556, Mar. 2014. doi: 10.1016/j.jallcom.2013.12.140.

[17] A. Valla, P. Carroy, F. Ozanne, and D. Muñoz, "Understanding the role of mobility of ITO films for silicon heterojunction solar cell applications," *Sol. Energ. Mat. Sol. C.*, vol. 157, pp. 874-880, Aug. 2016. doi: 10.1016/j.solmat.2016.08.002.

[18] K. Hong, S. Y. Yang, C. Yang, S. H. Kim, D. Choi, and C. E. Park, "Reducing the contact resistance in organic thin-film transistors by introducing a PEDOT:PSS hole-injection layer," *Org. Electron.*, vol. 9, no. 5, pp. 864-868, Jun. 2008. doi: 10.1016/j.orgel.2008.06.008.

[19] S. M. Gali, G. D. Avino, P. Aurel, G. Han, Y. Yi, T. A. Papadopoulos, V. Corpoceanu, J. L. Bredas, G. Hadziioannou, C. Zannoni, and L. Muccioli, "Energetic fluctuations in amorphous semiconducting polymers: impact on charge-carrier mobility," *J. Chem. Phys.*, vol. 147, no. 13, pp. 134904, Oct. 2017. doi:10.1063/1.4996969.

[20] E. Talgorn, R. D. Abellon, P. J. Kooyman, J. Piris, T. J. Savenije, A. Goossens, A. Houtepen, and L. D. A. Siebbeles, "Supercrystals of CdSe quantum dots with high charge mobility and efficient electron transfer to TiO_2," *ACS Nano*, vol. 4, no. 3, pp. 1723-1731, Sep. 2017. doi: 10.1021/nn901709a.

[21] N. Kirkwood, B. Singh, and P. Mulvaney, "Enhancing quantum dot LED efficiency by tuning electron mobility in the ZnO electron transport layer," *Adv. Mater. Interfaces*, vol. 3, pp. 1600868-1-7, 2016. doi: 10.1002/admi.201600868.

[22] K. S. Kim, S. M. Kim, H. Jeong, M. S. Jeong, and G. Y. Jung, "Enhancement of light extraction through the wave-guiding effect of ZnO sub-microrods in InGaN blue light-emitting diodes," *Adv. Funct. Mater.*, vol. 20, no. 7, pp. 1076-1082, Mar. 2010. doi:10.1002/adfm.200901935.

[23] D. A. Neamen, *Semiconductor physics and devices: basic principles*. New York, NY, USA: McGraw-Hill, 2012, pp. 311-340. doi: 10.1016/S1369-7021(06)71498-5.

[24] H. J. Jhuo, P. N. Yeh, S. H. Liao, Y. L. Li, S. Sharma, and S. A. Chen, "Inverted perovskite solar cells with inserted crosslinked electron-blocking interlayers for performance enhancement," *J. Mater. Chem. A.*, vol. 3, pp. 9291-9297, Mar. 2015. doi: 10.1039/c5ta01479d.

[25] C. A. Leatherdale, and M. G. Bawendi, "Observation of solvatochromism in CdSe colloidal quantum dots, " *Physical Review B.*, vol. 63, no. 16, pp. 165315, Apr. 2001. doi: 10.1103/PhysRevB.63.165315.

[26] J. I. Hong, P. Winberg, L. S. Schadler, R. W. Siegel, "Dielectric properties of zinc oxide/low density polyethylene nanocomposites," *Mater. Lett.*, vol. 59, no. 4, pp. 473-476, Oct. 2005. doi:10.1016/j.matlet.2004.10.

0741-3106 (c) 2019 IEEE. Personal use is permitted, but republication/redistribution requires IEEE permission. See http://www.ieee.org/publications_standards/publications/rights/index.html for more information.